Analysis of underwater vibration of a torpedo-shaped structure subjected to an axial excitation

Jie Pan (1), David Matthews (2), Heye Xiao (1), Andrew Munyard (2), and Yuxing Wang (1), Ming Jin (1), Wei Liu (1) and Hongmei Sun (1)

(1) School of Mechanical and Chemical Engineering, University of Western Australia, Crawley WA 6009, Australia
(2) Defence Science and Technology Organisation, HMAS Stirling, Rockingham WA 6958, Australia

ABSTRACT

This paper summarizes the experimental results of underwater vibration of a torpedo-shaped structure under axial excitation. Through the comparison of the vibration of the structure in water with that in air, we have found that the peak frequencies and corresponding mode shapes of the wet structure may differ significantly from those of the dry structure. This paper explains the change of the modal characteristics of the wet in terms of the coupling of the dry structural modes. The possible links between the wet and dry modes of the same structure are further illustrated by the vibration modelling of a fluid-loaded plate.

INTRODUCTION

The underwater vibration and sound radiation characteristics of structures have been an important topic of research, because of the application of underwater survey/operation vehicles and associated concern of their noise signature and impact of their underwater sound radiation on the ocean environment [1, 2]. The fluid loading makes the analysis of vibration and sound radiation of submerged structure less straightforward due to its heavy mass density, viscous loss and better impedance match with the structure.

Previous work on the experimental investigation [3] into the vibration and sound radiation of a torpedo-shaped structure in air aimed at searching for experimental evidence to (1) support the results from FEA modelling [4], (2) identify new mechanisms/structural details, which are important to the structural vibration and sound radiation but overlooked in the existing models, (3) provide the resonance frequencies, mode shapes and radiation directivity of the structure in air (which are close to the "in vacuum modes") for the understanding of the underwater testing results, which are often limited by a few sensors and environmental constraints.

Indeed, the results obtained from in-air measurement demonstrated some mode shapes which were not previously predicted due to complex coupling between the hemispherical dome (at the front end of the structure), the middle cylindrical section and the conical section (at the rear end of the structure), and due to the asymmetrical property of the practical structure. It was also found that the sound radiation directivities corresponding to these modes are affected significantly by the asymmetrical property.

The purpose of this paper is to report the experimental results of underwater vibration of a torpedo-shaped structure, whose vibration characteristics in air have been investigated in detail [3]. The first part of the paper covers description of experimental setup. Then the test results of underwater vibration are presented and compared with their counterparts measured in air. The analysis and discussion of the results focuses on the understanding of the effect of fluid loading on the modal response of the structure with respect to a unit input force.

DESCRIPTION OF EXPERIMENT

Test structure

The torpedo-shaped structure of the experiment (Figure 1) includes three components, a hemispherical dome, a cylinder and a conical shell, joined together via screw connections and with o-rings for water seal. A mechanical shaker was used to apply an axial force at the centre of a disk welded inside of the cone. Mass blocks were added at two locations of the cylinder to counteract the buoyant force and balance the structure in the horizontal plane.

The structure was suspended, respectively, by an aluminium frame in water, and by a metal cable in air (Figure 2) through two bull-eyes welded on the top of the cylinder.

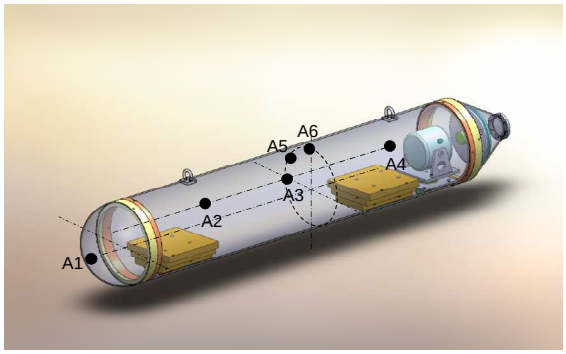

Figure 1. The torpedo-shaped structure for the experiment and location of six accelerometers

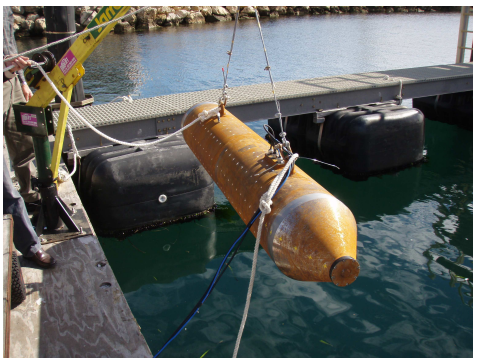

Figure 2. Torpedo-shaped structure in air before underwater test

Vibration measurement system

Inside the torpedo shaped structure, six IEPE accelerometers (Figure 1) are mounted, respectively, on the hemispherical dome (A1), the side wall (A2-A4), and along the circumferential direction of the cylinder (A5 and A6). An impedance head is inserted between the shaker and the disk in the conical shell, providing the driving force and acceleration. The accelerations measured by the six accelerometers are spatially averaged to give the structural velocity squared. Referenced with the driving force, it proximately represents the overall vibration per unit force:

$$\frac{< v^2(\omega) >}{F^2(\omega)} = \frac{1}{6\omega^2 F^2(\omega)} \sum_{i=1}^{6} a_i^2(\omega) \qquad (1)$$

where a_i is the measured acceleration at the ith location of the structure. It should be mentioned that a more suitable reference level for the comparison of the vibration response is input power. As shown in Figure 1 that the mechanical shaker, in fact, has two paths in exciting the structure. The direct path is through the impedance head and acting on the disk within the conical shell. As the shaker is rigidly clamped to the rear part of the cylinder, the reaction force resultant (axial force and bending moment) may exist in the cylinder structure underneath the shaker. It is also found that the input mobility at the conical disk does not carry much information of the structural resonances, except some weak response at the first two peak frequencies. This indicates that the conical disk might be too stiff and the true energy transmission path is not through there. It is more likely, the cylinder underneath the shaker is the portion where the vibration power is transmitted. As such input power is difficult to measure, and the reaction force is the cause of generating such power, we thus decided to use the driving force as the input reference.

Also included in the structural cavity are the signal conditioning box for the IEPE accelerometers, charge amplifiers for the impedance head and a DAQ card to locally sample all the acceleration and force signals. The digital signals were sent to the onshore PC through an Ethernet Cat5e cable. A 24V DC power was supplied to the signal conditioning box and charge amplifiers. A power amplified signal was provided from land to the mechanical shaker in the structural cavity.

To increase the signal to noise ratio for underwater test, stepped sine signals at a fixed frequency were used to excite the structural vibration. The structure was excited at each frequency for 4 seconds; 1 second length of data was sampled after the initial transient decayed completely. Then standard FFT analysis was applied to the data and the amplitude and phase of the signal were extracted at the frequency of interest. The vibration at the six locations, the input force and acceleration of the structure were measured in air and in water for comparison purpose.

RESULTS AND DISCUSSION

Structural Vibration

The purpose of comparing the test results between the in air test (dry) and in water test (wet) of the same structure is to search for the possible similarity between the dry and wet structural modes. Such a search may not only lead to an understanding of the wet modes in terms of the dry modes, but also allow a possibility of using the dry modes (which can be obtained by in land experiment) to predict the wet modes and their responses (whose measurement are often difficult).

For this purpose, we first show in Figure 3 the spatial averaged velocity of the structural tested in air and in water with respect to the driving force. These curves approximately represent the structural vibration energy due to one unit of driving force, and carry the overall resonance characteristics of the structural vibration.

The comparison of the two curves demonstrates the change in vibration response of a wet structure as expected. The curve of the wet structure resembles that of the dry structure, but with its peak frequencies shifted towards the low frequency range, indicating the mass loading effect of the fluid. The bandwidth and peak value of the wet curve at the "higher" frequencies become broad and lower, indicating the effect of increased energy loss (damping) when a structure is submerged in water. The shift of the peak frequencies of the first 8 peaks in Figure 3 are listed in Table 1, where we can observe the increased frequency shift (towards the low frequency) of the 7th and 8th peaks, which can be explained by increased fluid mass loading effect at higher frequencies. We are not able to determine the 5th peak frequency of the wet structure because the response is over damped. The 3rd peak of the dry structure is not identified.

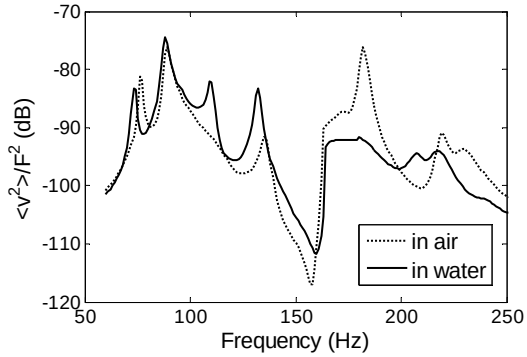

Figure 3. Spatial averaged vibration with respect to input force

The apparent similarity of the averaged structural velocities between the dry and wet tests posed the question as whether the mode shapes of the wet structural modes (at the peak frequencies) are also similar to those of the dry structural modes. Unfortunately, the wet mode shapes are not available

as we only have the measured responses of the wet structure at 6 locations.

Table 1 Frequencies of the first 8 peaks

No.	*In Air (Hz)*	*In Water(Hz)*	*% Difference*
1	76	74	2.6%
2	90	88	2.2%
3	-	109	-
4	136	132	2.9%
5	172	-	-
6	182	180	1.1%
7	220	207	5.9%
8	229	218	4.8%

Nevertheless, the vibrations with respect to the input force at each of these locations are shown in Figure 4. They start to show the complexity of fluid loaded structural vibration. Most importantly, we observe the change of the mode shapes of the wet structure from that of the dry structure at the peak frequencies due to fluid-loading effect.

In air, the first two peaks have similar mode shapes. They result from the coupling of the structural mode with the suspension cable. At the 2nd peak frequency (90Hz), most system energy is in the structure. Thus the peak is dominated by a "structural controlled mode" and it will significantly contribute to the sound field radiation. The vibration distribution at this peak frequency is measured by using multiple accelerometers as described in ref [3] and displayed in Figure 5. It should be noted that the cylinder is connected with the cone at $length = 0$.

As described in reference [1], the high level vibration at the hemisphere dome indicates a monopole-like modal sound radiation towards the front part of the structure. The measured vibration at 5 locations of the wet structure (except at location 3) is consistent with the mode shape of the dry structure at the 2nd peak frequency at regions of measurement. At location 2 for the 2nd peak, however, a significant level difference in vibration between the wet and dry structure is observed. At this location, the response of the dry structure is very low as the location is far away from where large vibration occurred. However the vibration of the wet structure still shows a strong resonance response at the 2nd peak.

This result demonstrates that the fluid loading may have significantly changed the vibration distribution of the wet structure in the section of the cylinder close to the hemisphere dome. At this peak frequency, the fluid loading may have extended the large vibration area from the dome to the front part of the cylinder. Such a change of the vibration pattern may lead to some increase in the sound radiation in the front part of the structure.

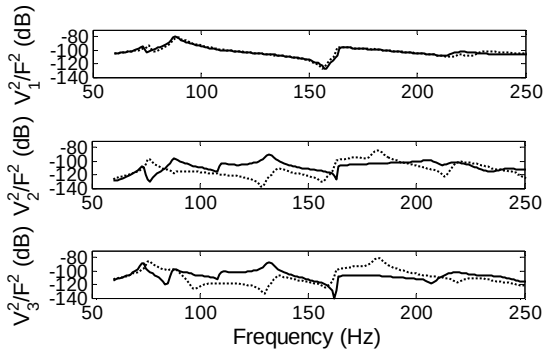

Figure 4a. Vibration at locations 1-3 with respect to the input power (solid curves: in water; dashed curves: in air)

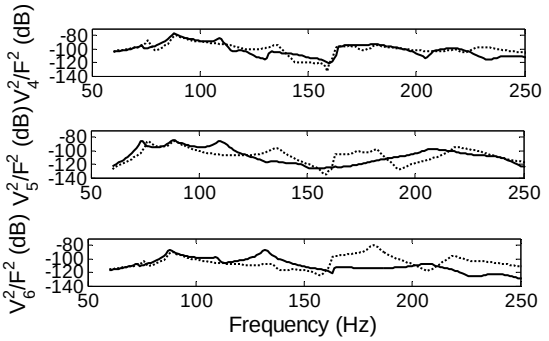

Figure 4b. Vibrations at locations 4-6 with respect to the input power (solid curves: in water; dashed curves: in air)

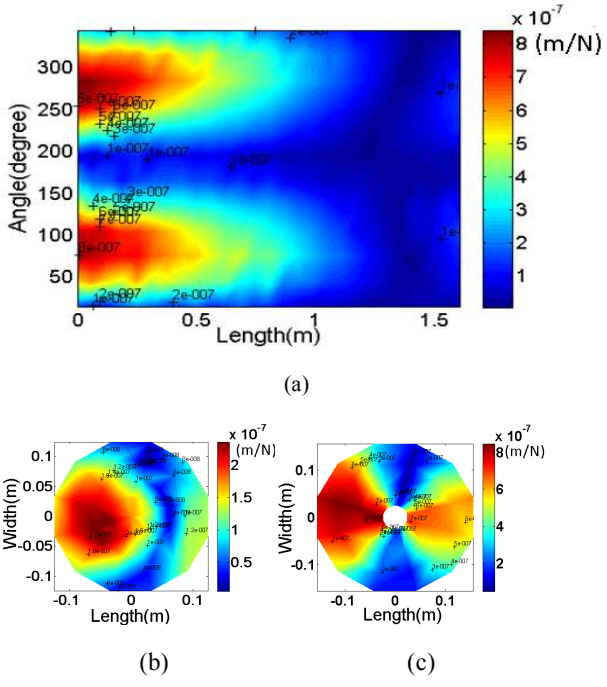

Figure 5. Vibration distribution of the torpedo-shaped structure measured in air and at the 2nd peak frequency; (a) distribution in the cylinder section, (b) distribution in the hemispherical dome, and (c) distribution in the conical shell.

A big difference between the wet and dry structural vibration is found at the 4th peaks of curves (136Hz in air, 132Hz in water). This observation suggests that the corresponding mode shapes could be totally different although the frequencies of the peaks are only shifted by 3Hz. Table 2 summarizes the corresponding level differences at the six locations. If the mode shapes corresponding to the 4th peaks of the wet and dry structure are the same, a consistent level difference would have been observed.

Table 2 Levels at the 4th peak frequency

Location	*In Air (dB)*	*In Water (dB)*	*Difference (dB)*
1	-105	-105	0
2	-111	-90	-11
3	-107	-88	-19
4	-94	-104	10
5	-95	-117	-22
6	-107	-87	20

Figure 6 shows the radiated sound pressure (with respect to the driving force) measured 2m away from the centre of the structure and right in front of the dome. Although the peak sound pressure at 73Hz, 88Hz, 109Hz and 132Hz can be correlated to the vibration peak frequencies of the wet structure (see Figure 3), some interesting sound radiation features are observed here.

A rather strong radiation peak can be identified at 93Hz. This peak is very close to that (88Hz) of the strong vibration mode (with maximum level at the dome) of the structure. The slight shift of the peak frequency seems to suggest that the mode may have much larger radiation efficiency slightly above the natural frequency of the structure. The similar study of sound radiation of plates was reported by Wallace [5].

Another strong peak sound radiation occurred at 168Hz. This peak may be related to the overdamped 5th peak of the wet structure response (see Table 1). It is noted that the underwater testing environment is not perfectly anechoic. The effect of sound reflection from the water surface (5m above) and seabed (5m below), and shore on the measurement of sound radiation is yet to be investigated, although at the measurement location the direct sound is pretty strong.

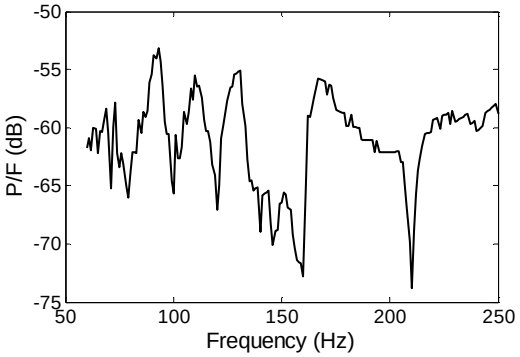

Figure 6. Radiated sound pressure with respect to the driving force measured 2m from the centre of the underwater structure and in front of the spherical dome

Vibration Analysis

To understand the vibration characteristics of the wet structure using modal characteristics of the dry structure, the fluid loading effect on a semi-finite elastic plate (finite in x-direction, infinite in z-direction) is analysed here. The result of this analysis may shine some light on the above experimental observations.

A two-dimensional finite plate of thickness h, coupled with fluid in the region of $y \geq 0$, is shown in Figure 7. The plate is simply supported at $x = 0$ and $x = L$ by rigid baffles of infinite size and is excited by a line force $F_o e^{-j\omega t}$ at $x = x_o$.

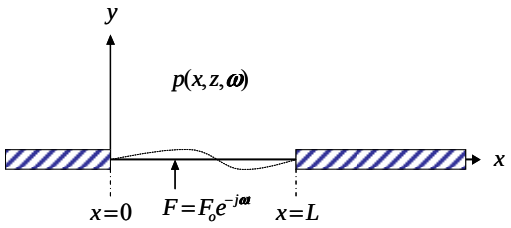

Figure 7. A fluid-loaded finite plate in an infinite baffle

We express the displacement of the plate by the dry mode shapes of the plate vibration:

$$w(x,\omega) = \sum_n w_n \sin(k_n x) \qquad (2)$$

where $k_n = n\pi / L$. Using the wavenumber analysis of the plate and sound wave equations [6], the final coupled equations of the coefficients of the plate displacement are given below for analysis:

$$(k_n^4 - k_p^4) w_n - \mu k_p^4 \sum_{n'} I_{nn'} w_{n'} = \frac{2F_o}{DL} \sin k_n x_o \qquad (3)$$

where $\mu = \rho_o / \rho_p h$ represents fluid-loading and $k_p = (\rho_p h \omega^2 / D)^{1/4}$ is the flexural wavenumber of the plate in a vacuum. Other system parameters are $D = Eh^3 / [12(1-\nu^2)]$ being the plate's bending stiffness, and ρ_p, E and ν respectively the density per unit area, Young's modulus and Poisson's ratio of the plate. The internal damping of the plate is included in the system model by using a complex Young's modulus $E^* = E(1 + j\eta)$, where η is the structural loss factor. The important terms in Equation (3) are the modal coupling factors, which represent the interaction between n^{th} and n'^{th} dry modes through their near field sound radiation

$$I_{nn'} = \frac{1}{\pi L} \int_{-\infty}^{\infty} \frac{\phi_{n'}(\gamma_x) \phi_n^*(\gamma_x)}{\gamma_y} d\gamma_x \qquad (4)$$

where $\phi_{n'}(\gamma_x) = \int_0^L \sin(k_{n'} x) e^{-j\gamma_x} dx$. $\gamma_y = \sqrt{\gamma_x^2 - k_o^2}$ is the acoustic wavenumber of the sound pressure in the y direction,

and $k_o = \omega / c_o$ the acoustical wavenumber in the fluid and γ_x represents the wavenumber in the x direction. The contribution of the self-modal loading ($n' = n$) and cross-modal loading to the plate response can be estimated by $\mu = \rho_o / \rho_p h$. For a steel plate with the thickness of 10mm, this ratio is negligibly small for air loading such that the coupling due to near field sound radiation can be ignored. As a result, the displacement response of the dry plate can be approximated as

$$w(x,\omega) \approx \sum_n \frac{2F_o \sin(k_n x_o)\sin(k_n x)}{DL(k_n^4 - k_p^4)}. \quad (5)$$

A numerical comparison between Equations (5) and (3) showed that the air loading only adds extra radiation damping to the plate vibration. The response of the dry plate at the n^{th} peak frequency is dominated by the n^{th} "in-vacuum" mode of the plate.

If the plate is loaded with water, the fluid-loading parameter increases by nearly 1000 times, which makes the coupling term in Equation (3) important. For this case, the peak response of the wet plate calculated by Equations (2) and (3) will consist of several modal coefficients of the dry structure, which result from the coupling between those dry modes.

To generate numerical evidence, we have used the plate and water parameters as listed in Table 3. The driving location of the point line force is $x_o = 0.33m$.

Table 3 Water and plate parameters for simulation

Water	*Plate*
$\rho_o = 1000kg/m^3$	$\rho_p = 7800kg/m^3$
$c_o = 1460m/s$	$E = 21.6\times10^{10}Pa$
	$\nu = 0.3$
	$\eta = 0.01$
	$h = 0.01m$
	$L = 1.2m$

In Figure 8, we compare the spatial averaged velocities (per unit force) of the wet and dry plates. The frequency shift (towards the low frequency) and increase of modal damping of the structural modes are evident. For the convenience of the comparison between the dry and wet mode shapes at the peak frequencies, the first 4 peak frequencies are listed in Table 4.

Indeed, we observed that the vibration patterns of the plate in air (see Figure 9) at the first 4 peak frequencies are very close to the "in vacuum" mode shapes of the plate. The fluid loading effect on the mode shape at the first peak frequency seems to be negligible, although it significantly altered the peak frequency. This observation suggests that the cross mode coupling is not important to the response at the first peak frequency. The cross mode coupling plays an important role for altering the mode shapes from the second peak frequency and above. As shown in the second row of Figure 9a, the vibration amplitude in the range of $1/2 \le x/L \le 1$ becomes smaller than that in $0 \le x/L \le 1/2$. This is because of the coupling contribution of the first dry mode (see the bottom plate in Figure 10a) and its destructive interference in $1/2 \le x/L \le 1$ and constructive interference in $0 \le x/L \le 1/2$ with the second mode. It would be interesting to investigate the detailed mechanisms involved in the effect of fluid loading on the change of mode shapes. Work is underway to analyse the complex energy flow between the plate and water so that we can distinguish the components of mass/stiffness loading (imaginary energy flow) and fluid damping loss (real energy flow).

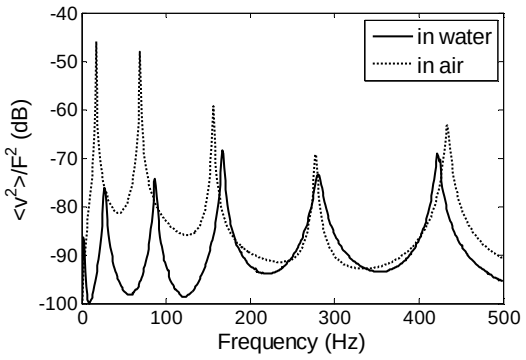

Figure 8. Spatial averaged plate vibration with respect to driving force

Table 4 Frequencies of the first 4 peaks of the wet and dry plate

No.	*In Air (Hz)*	*In Water(Hz)*	*% Difference*
1	17	2	88%
2	69	28	59%
3	156	87	44%
4	278	167	40%

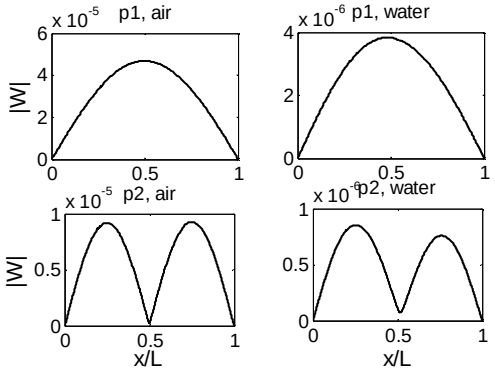

Figure 9a. Dry and wet mode shapes at the 1st and 2nd peak frequencies.

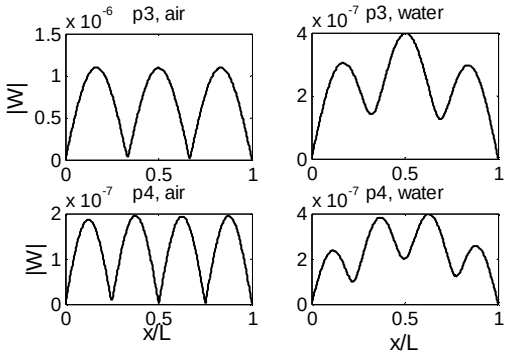

Figure 9b. Dry and wet mode shapes at the 3rd and 4th peak frequencies.

The fluid-loading shows a stronger effect on the shapes of the 3rd and 4th wet modes (see Figure 9b). It is interesting to note from the modal decomposition results in Figure 10b that the change in the shape of the wet mode at the n^{th} peak frequency largely involves the modal coupling with all the lower order modes ($n-1, n-2, ..., 1$) and the mode immediately above ($n+1$). The involvement of the first and second in-vacuum modes exists in response of the wet structure at the second peak (see the lower plate of the Figure 10a), although their magnitudes are relatively small in the figure.

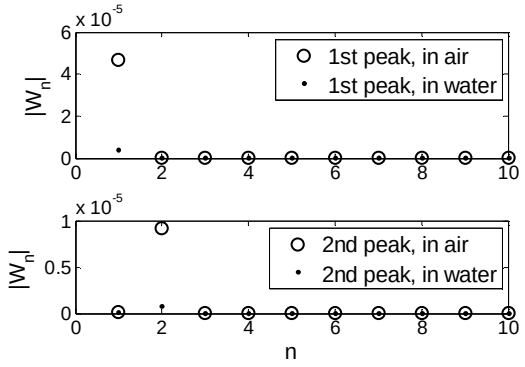

Figure 10a. Coefficients of the first 10 dry modes for the response of the plate at the 1st and 2nd peak frequencies

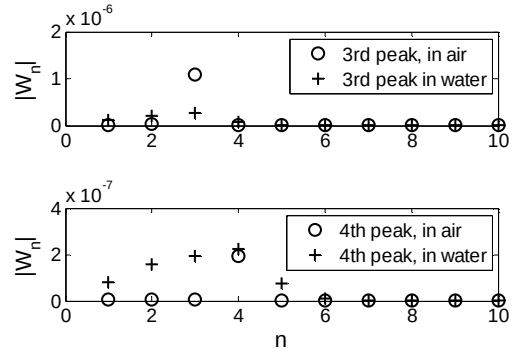

Figure 10b. Coefficients of the first 10 dry modes for the response of the plate at the 3rd and 4th peak frequencies

Although the fluid-loaded plate model assisted our understanding of the modal response of the wet torpedo-shaped structure, it is worthwhile to make the following comments in regard to the features of the fluid-loaded torpedo-shaped structure:

(1) Compared with the results to Figure 8, the shift in the peak frequency of the fluid-loaded torpedo-shaped structure (see Figure 3) is relatively small. It may be due to geometric shapes of the shell/dome/cone which makes the change of natural frequency difficult. It may also be due to the excessive mass loading of the payloads which makes the mass loading effect of the water less significant. Once again, the results shown in Figure 8 are based on the thin plate theory and the transverse stiffness is relatively low when compared with that of the torpedo-shaped structure.

(2) A challenging question is how to use the measured modal characteristics of the dry structure (such as the torpedo-shaped structure) for predicting the vibration and sound radiation of the same structure when it is placed in water. The example of the fluid-loaded plate seems to suggest the expansion of the vibration of the wet structure using the mode shape functions of the dry structure. Then the fluid loading effect may be taken into account using the coupling between the dry modes and their near field sound radiation [7]. The aim is to obtain the modal coupling equations similar to Equation (3) using BEM modelling similar to what has been implemented in BEM software packages. The only difference is that here the in-vacuum modes are obtained as dry modes experimentally.

CONCLUSIONS

The underwater vibration of a torpedo-shaped structure subject to an axial excitation is investigated experimentally. By comparing the peak frequencies and vibration responses of the wet and dry structures, we conclude that the modal shape functions of the wet structure could significantly differ from those of the dry structure. An example of the vibration of fluid-loaded plate is used to explain the change of peak frequencies and mode shapes of the wet structure in terms of the coupling of the dry structural modes through their near field sound radiation. This interpretation of the vibration of a wet structure allows a possibility of using measured dry structural modal characteristics (which is relatively easier to obtain) to predict those of the wet structure.

ACKNOWLEDGEMENTS

We thank Dr Andrew Gussomi for proof reading this manuscript and his useful comments. We also thank Gary Chandler for his technical support during the field measurement.

REFERENCES

[1] G. Griffiths, P. Enoch, and N. W. Millard, "On the radiated noise of the autonomous underwater vehicle", Journal of Marine Science, 58: 1195–1200. (2001)

[2] Cuschieri J., "Estimation and measurement of the acoustic signature of unmanned surface and underwater vehicles", J. Acoust. Soc. Am., Vol. 127, No. 3, Pt. 2, March, pp. 1813, (2010).

[3] Liu W., Pan J. and Mathews D., "Measurement of sound radiation from a torpedo-shaped structure subject to an axial excitation", Proceedings of 20th International Congress on Acoustics, Sydney, Australia. (2010).

[4] Merz S., Kinns R. and Kessissoglou N., "Structural and acoustic responses of a submarine hull due to propeller forces" Journal of Sound and Vibration 325, 266–286, (2009).

[5] Wallace C. E., "Radiation resistance of a rectangular panel", J. Acoust. Soc. Am. 51, 946-952, (1972).

[6] Chang Y. M. and Leehey P., "Acoustic Impedance of Rectangular Panels" Journal of Sound and Vibration 64(2), 243–256, (1979).

[7] Zhoua Q. and Joseph P.F.,"A numerical method for the calculation of dynamic response and acoustic radiation from an underwater structure" Journal of Sound and Vibration, 283, 853–873, (2005).